ELSEVIER

Shell gap reduction in neutron-rich $N = 17$ nuclei

A. Obertelli [a,*], A. Gillibert [a], N. Alamanos [a], M. Alvarez [a,1], F. Auger [a], R. Dayras [a], A. Drouart [a],
G. de France [b], B. Jurado [b,2], N. Keeley [a], V. Lapoux [a], W. Mittig [b], X. Mougeot [a], L. Nalpas [a],
A. Pakou [c], N. Patronis [c], E.C. Pollacco [a], F. Rejmund [b], M. Rejmund [b], P. Roussel-Chomaz [b],
H. Savajols [b], F. Skaza [a], Ch. Theisen [a]

[a] *CEA-SACLAY DSM/DAPNIA/SPhN, F-91191 Gif-sur-Yvette, France*
[b] *GANIL BP 5027, F-14076 Caen Cedex 5, France*
[c] *Department of Physics, The University of Ioannina, 45110 Ioannina, Greece*

Abstract

The spectroscopy of ^{27}Ne has been investigated through the one-neutron transfer reaction ^{26}Ne$(d, p)^{27}$Ne in inverse kinematics at 9.7 MeV/nucleon. The results strongly support the existence of a low-lying negative parity state in ^{27}Ne, which is a signature of a reduced sd–fp shell gap in the $N = 16$ neutron-rich region, at variance with stable nuclei.
© 2005 Elsevier B.V. Open access under CC BY license.

It has already been shown that the sequence of nuclear magic numbers may change from stability to the drip lines. This is the case for the disappearance of the $N = 20$ magicity in the neutron-rich sodium and magnesium isotopes [1,2]. New magic numbers may also appear: $N = 16$ has been suggested to be magic near the neutron drip line, both theoretically [3–5] and experimentally [6,7]. This may arise from an enhancement with isospin of the gap between the $s_{1/2}$ and $d_{3/2}$ subshells of the sd neutron shell [4] and/or proton–neutron correlation effects [8].

The study of the single particle excitations in $N = 17$ isotones is well suited to determine the spacing between the $d_{3/2}$ subshell and the fp shell. In a first approximation, the $N = 17$ isotones can be considered as $N = 16$ nuclei with an extra

neutron in the $d_{3/2}$ subshell of the sd shell. Single particle excitations where the $d_{3/2}$ neutron is promoted to the fp shell, result in negative parity excited states. The most bound $N = 17$ isotones ^{35}Ar, ^{33}S and ^{31}Si have high lying negative parity states at excitation energies of ~ 3.5 MeV. However, excitation energies below 1.5 MeV are suggested for ^{29}Mg [9,10] (see Fig. 1). This is surprising for two reasons: (i) the energies of these states are unexpectedly low compared to the other $N = 17$ isotones and (ii) the energy of the $3/2^-$ state is below the $7/2^-$ state in contradiction with the ordering of the fp orbitals at stability. Intruder states from the fp shell have recently been observed in ^{28}Na [11] in accordance with an earlier sd–fp shell model calculation [12]. The next $N = 17$ isotone is ^{27}Ne for which very little information is available: two levels at 750 keV and 900 keV are reported in [13] from the γ-ray spectroscopy of ^{27}Ne via ^{9}Be$(^{36}$S, ^{27}Ne$\gamma)$X at 77 MeV/nucleon; only one transition at 870(16) keV was observed in [14] where ^{27}Ne was produced through the one neutron removal ^{12}C$(^{28}$Ne, ^{27}Ne$\gamma)$X at 46 MeV/nucleon. Neither spin nor parity assignments have been made in the aforementioned studies.

* Corresponding author.
  E-mail address: aobertel@cea.fr (A. Obertelli).
[1] Present address: Departamento de FAMN, Universidad de Sevilla, E-41080 Sevilla, Spain.
[2] Present address: Centre d'Etudes Nucléaires de Bordeaux-Gradignan, F-33175 Gradignan Cedex, France.
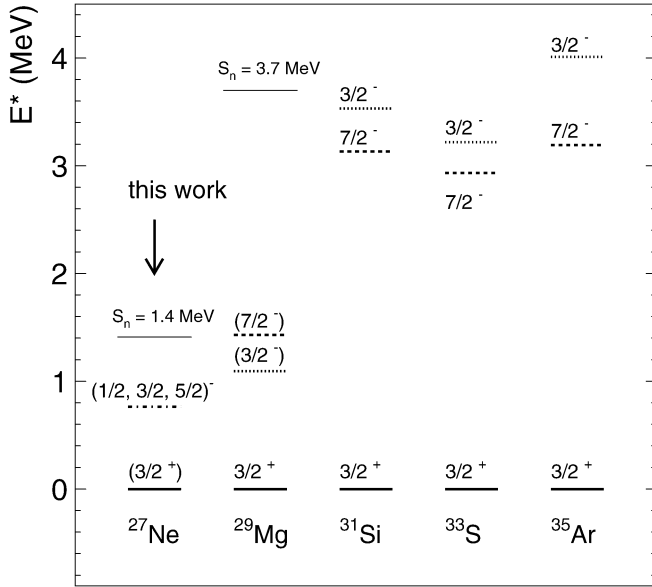
Fig. 1. Systematics of experimental low-energy negative-parity states for odd $N = 17$ nuclei from ^{35}Ar to ^{27}Ne.

In this Letter, we report on results from a ^{26}Ne$(d, p)^{27}$Ne experiment in inverse kinematics performed at 9.7 MeV/nucleon. Due to a possibly large level density in ^{27}Ne, a γ ray coincidence method has been used. The ^{26}Ne beam was produced by the ISOL method using the SPIRAL facility of GANIL (Grand Accélérateur National d'Ions Lourds). A ^{36}S primary beam at 77.5 A MeV was fragmented and stopped in a thick carbon target. The ISOL products were accelerated by the CIME cyclotron tuned for ^{26}Ne^{5+}, and a pure ^{26}Ne beam was delivered at 9.7 MeV/nucleon with an intensity of 3000 particles per second. Due to the low beam intensity, it was necessary to use a target thick enough to balance the small one neutron transfer cross sections. We used a solid cryogenic D$_2$ target (17 mg cm^{-2}) [15], developed at GANIL, thicker than a CD$_2$ target by a factor 3 for the same energy loss. Its homogeneity was controlled to be better than 2.5%. Due to the target thickness, recoiling protons were not measured; also no conclusive angular distribution of the ejectiles was obtained. A possible contamination from the Mylar windows of the target and the ^{26}Ne$(^{12}$C, ^{11}C$)^{27}$Ne channel is hindered by the strongly negative Q value ($Q = -17.3$ MeV) compared to the (d, p) channel ($Q = -0.8$ MeV) and the small thickness of the Mylar windows (24 μm). The beam-like reaction products and the outcoming beam were detected in the focal plane of the VAMOS magnetic spectrometer [16], allowing an identification of ejectiles and a counting rate measurement of reaction products and ^{26}Ne beam particles. Both singles in VAMOS and events in coincidence with γ rays were detected. Photons were measured in the EXOGAM spectrometer [17] surrounding the target (see Fig. 2). In the experiment, 11 clovers (8 EXOGAM clovers and 3 EUROGAM size detectors) were placed at distances varying from 11 to 17 cm from the center of the target. The detectors were placed on three angular rings: 4 at forward angles (45°), 3 at backward angles (135°) and 4 at 90°. Each clover consisted of 4 × 4-fold segmented germanium crystals. The in-
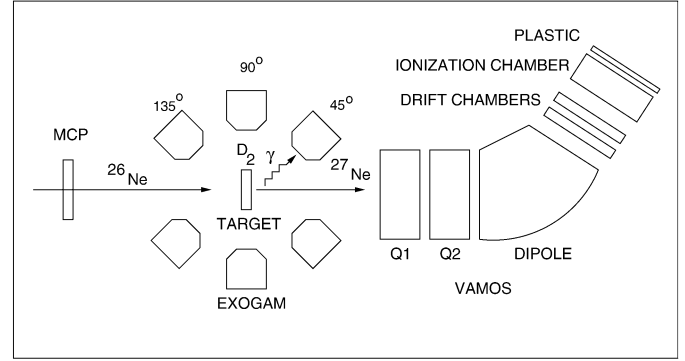

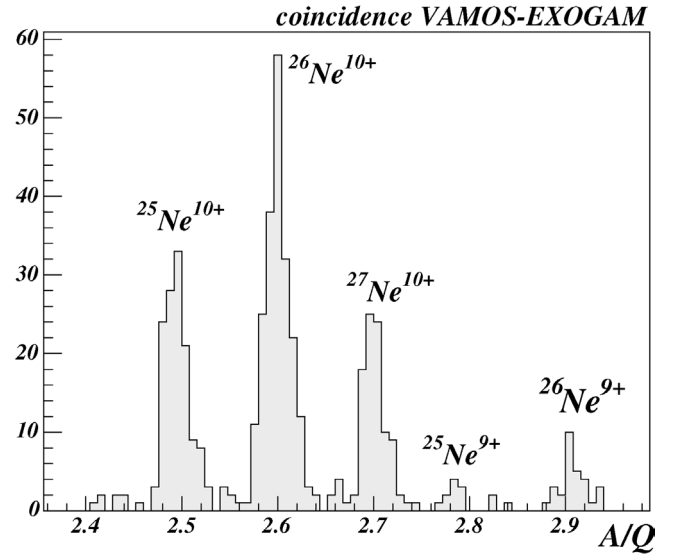Fig. 2. Scheme of the experimental setup in the VAMOS vault.

Fig. 3. A/Q identification for neon isotopes. Events in VAMOS in coincidence with a photon detected in EXOGAM are shown.

trinsic energy resolution of the whole system was measured to be 2.6 keV (FWHM) at 1332 keV, and the corresponding photopeak efficiency was estimated to be 4.8%. To identify ^{27}Ne^{10+} beam-like ejectiles in the focal plane of VAMOS, we used combinations of the following parameters: (i) the time of flight (ToF) between a microchannel plate device (MCP) before the target and the plastic scintillator of VAMOS, (ii) the energy loss ΔE in the ionization chamber of VAMOS and (iii) the horizontal position X_f on the focal plane of VAMOS measured by two drift chambers. The Z identification was performed with the ΔE–ToF plot. A direct A/Q assignment was done *via* the ToF–X_f plot, for $Z = 10$ ejectiles in coincidence with EXOGAM as shown in Fig. 3: ^{27}Ne^{10+} is clearly identified from the other neon isotopes. Results for the spectroscopy of ^{25}Ne and ^{26}Ne will be presented elsewhere.

The resulting γ-ray spectrum of ^{27}Ne is shown in Fig. 4, with events of multiplicity 1 and add-back corrected events of multiplicity 2 in two adjacent crystals. The photons are emitted in flight, which requires a Doppler correction very sensitive to the relative velocity $\beta = v/c$ of the ejectile, c being the speed of light. Due to the target thickness, the ^{26}Ne beam is slowed down from $\beta = 0.142$ to $\beta = 0.090$. As the reaction vertex in
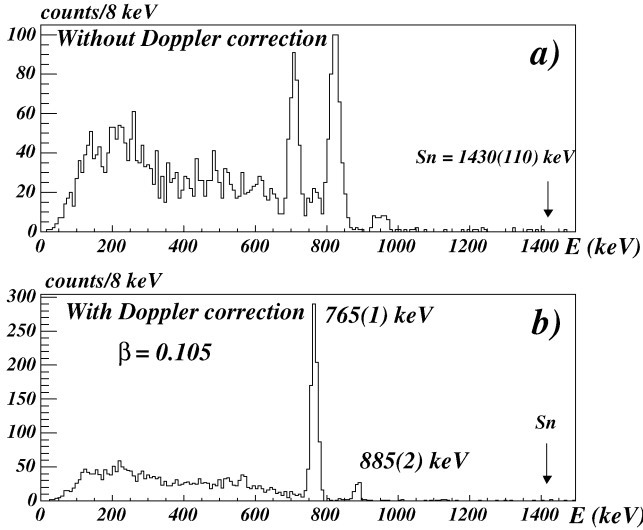
Fig. 4. Energy spectrum of photons measured in coincidence with ^{27}Ne without (a) and with (b) Doppler correction. The Compton edge of the 765 keV transition is at 573 keV, visible on the spectrum (b).

Fig. 5. Experimental level scheme of ^{27}Ne compared to USD predictions.

the target is not reconstructed, only the mean value of the velocity may be used. For ^{27}Ne and the (d, p) channel, a mean velocity $\beta = 0.105$ was adopted, for which the measured energies are equally well corrected at forward and backward angles. The effect of the Doppler shift is visible for the 765 keV transition in Fig. 4 a), without Doppler correction: the transition is split into three peaks corresponding to the three angular rings of γ detectors. The peak measured by the 90 degree detectors is much smaller due to the shadowing of the cryogenic target holder. Two peaks are visible on the Doppler corrected spectrum (Fig. 4b): one at 765(1) keV, and a weaker one at 885(2) keV. The widths, respectively 21(1) keV and 14(2) keV (FWHM), are mainly due to the uncertainty in the velocity $\Delta\beta/\beta = \pm 20\%$ of ^{27}Ne at the reaction vertex and the solid angle aperture of the segments for the Doppler correction. These widths are compatible with the expected value 15 keV (FWHM) obtained from a GEANT [18] simulation. It is unlikely that these two low energy transitions are in coincidence even if this scenario cannot be completely excluded: (i) the sum of the two energies, 1650(3) keV, is greater than the neutron separation energy $S_n = 1430(110)$ keV [19] by 2σ and is too low to favor γ decay against neutron emission, (ii) we found no event corresponding to a real time coincidence between these two peaks. Therefore, we assign these two transitions to two bound excited states in ^{27}Ne at excitation energies of 765 keV and 885 keV. We did not find evidence for a transition at $E_\gamma = 120$ keV, connecting these two states. This may be due partly to the importance of the Compton background at low γ energy, partly to selection rules which would favour the direct decay to the ground state rather than the cascade through the 765 keV state. Taking into account the efficiencies, the background at 120 keV and the number of events detected at 885 keV, a 20% upper limit for the branching ratio τ of the decay to the 765 keV state is found. This estimation takes into account the threshold effects at 120 keV. The level scheme obtained is presented in the left part of Fig. 5. This level scheme of ^{27}Ne is confirmed by a re-
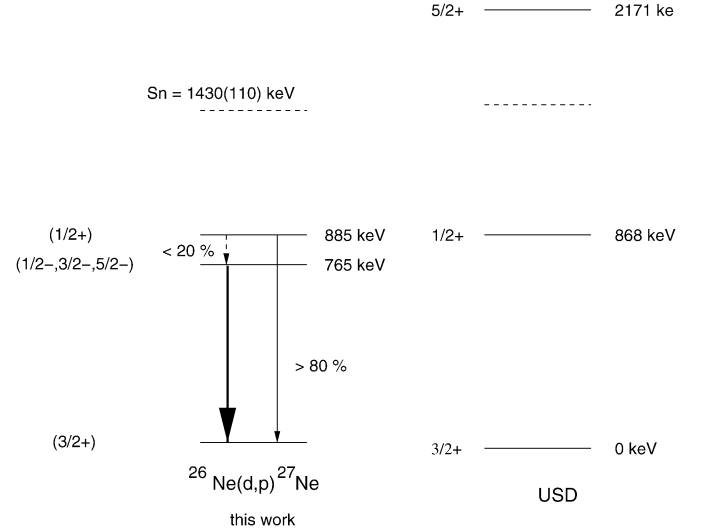
cent one-neutron knockout experiment performed at the NSCL (MSU) [20].

To determine the (d, p) cross sections to the different states of ^{27}Ne, the various photopeak efficiencies were estimated *via* GEANT simulations taking into account the complete geometry of the set-up. In order to get rid of A/Q efficiency dependency in cross section measurements, we considered only $Q = 10^+$ charge states for ^{26}Ne beam particles and ^{27}Ne ejectiles. The reliability of the simulated photopeak efficiencies was estimated, through source measurements, to be better than 90%. After efficiency correction, the ratio of the cross sections for the two excited states is

$$\frac{\sigma(765 \text{ keV})}{\sigma(885 \text{ keV})} = 8.8 \pm 1.3 \qquad (1)$$

for a branching ratio $\tau = 0\%$ from the 885 keV level to the 765 keV level. In the upper limit case of $\tau = 20\%$, the ratio is 6.8 ± 1.3. Assuming no undetected low energy bound state for ^{27}Ne, there is the following relationship between the total number $N_{27\text{Ne}}$ of ^{27}Ne ejectiles measured in the focal plane of VAMOS, the unknown number $N(\text{gs})$ of transfers to the ground state and the numbers of γ transitions corrected for efficiency $N(765)$ and $N(885)$

$$N(\text{gs}) = N_{27\text{Ne}} - N(765) - N(885). \qquad (2)$$

Thanks to the $\pm 5\%$ large momentum acceptance of VAMOS, there was no significant momentum cut for ^{26}Ne^{10+} and ^{27}Ne^{10+}. The resulting absolute cross sections $\bar{\sigma}_i$ integrated over the VAMOS angular acceptance (0°_{lab}–2.7°_{lab} due to a sharp geometrical cut by the beam tube between the target reaction chamber and the first quadrupole of VAMOS, corresponding to 0°_{cm}–65°_{cm}) are gathered in the left hand columns of Table 1. Limit values for $\tau = 0\%$ and $\tau = 20\%$ are reported. Due to the rather weak population of the 885 keV level, the effect of τ is small. The quoted uncertainties are mainly due to the statistical errors and a 10% uncertainty over the absolute photopeak efficiencies of EXOGAM.

Table 1
Calculated and experimental cross sections $\bar{\sigma}_i$ (see text). Two different scenarios have been considered for the first excited state X^- of ^{27}Ne: $\Delta l = 3$ (case a) and $\Delta l = 1$ (case b). Theoretical (USD) and experimental spectroscopic factors under the assumption of a 765 keV negative parity state are compared

E (keV)	Experiment			Theory					
	$\bar{\sigma}$ (mb)		C^2S	case a		case b		state	C^2S
	$\tau = 0\%$	$\tau = 20\%$		$\bar{\sigma}$ (mb)	Δl	$\bar{\sigma}$ (mb)	Δl		
0	4.6 (3.9)	4.6 (3.9)	0.2(2)	15	2	14	2	$3/2^+$	0.64
765	21.9 (2.3)	21.3 (2.3)	0.6(2)	37	3	41	1	X^-	1
885	2.5 (0.5)	3.1 (0.6)	0.3(1)	2	0	2	0	$1/2^+$	0.18

We now compare our data to theoretical calculations in order to investigate the possible spins and parities of the observed states. Shell model calculations performed with the USD interaction [21], restricted to the sd shell, predict only positive parity states with excellent results not only for nuclei close to the stability, but also for ^{26,27,28}Na [11,22,23] and ^{26}Ne low-lying states in the vicinity of ^{27}Ne. USD predicts only one excited state below S_n for ^{27}Ne: a $1/2^+$ state at 868 keV above the $3/2^+$ ground state (gs) (Fig. 5). That excitation energy is in good agreement with the two observed states. Assuming that USD qualitatively reproduces the positive parity states for ^{27}Ne, one of the two observed transitions should be a $1/2^+ \rightarrow 3/2^+$(gs) transition and then one of the two observed excited states might be a negative parity state. This assumption is supported by shell model calculations with the SDPF-M interaction [12,24] with predictions similar to those by the USD interaction for positive parity states and existence of low-lying negative parity states for ^{27}Ne [4, 25]. A low-lying negative parity state from the fp shell can be either a $1/2^-$, $3/2^-$, $5/2^-$ or $7/2^-$ state. Not all these possibilities are consistent with the present data. In the case of a $7/2^-$ state at 765 keV, the fastest decay to a $3/2^+$ gs implies a M2 transition. The Weisskopf estimates give at least a 10 ns half-life for such a transition, corresponding to a 30 cm path of flight in this experiment. According to a GEANT simulation, it should result in a strong difference in the counting rates of forward and backward Ge detectors and an asymmetry in the shape of the peaks in Fig. 4a. We do not observe any of these effects, which therefore excludes the $7/2^-$ state assumption. A 765 keV E1 transition is fast enough, so that the photon is emitted at the target position. Connected to a $3/2^+$ ground-state, the three other possibilities $1/2^-$, $3/2^-$ and $5/2^-$ are allowed. In the case of a X^- negative parity state at 765 keV and assuming the USD predictions for the ground state and the 885 keV excited state, we could expect a competition between a 120 keV E1 transition ($1/2^+ \rightarrow 1/2^-$) or ($1/2^+ \rightarrow 3/2^-$), and the direct 885 keV M1 transition to the ground state ($1/2^+ \rightarrow 3/2^+$). According to the Weisskopf estimates, a 885 keV M1 transition is 10 times faster than a 120 keV E1 transition. In the case of a 120 keV M2 transition ($1/2^+ \rightarrow 5/2^-$), the direct ($1/2^+ \rightarrow 3/2^+$) transition is clearly favored. Then, all $X^- = (1/2^-, 3/2^-, 5/2^-)$ possibilities are consistent with no observation of a 120 keV transition and an upper limit $\tau = 20\%$.

We can also compare the measured cross sections to CDCC (Continuum Discretized Coupled Channels) + CRC (Coupled Reaction Channels) calculations with the code FRESCO [26]. Among the different couplings between the $d + ^{26}$Ne and $p + ^{27}$Ne channels, the break-up of the deuteron is taken into account, as in [27]. For ^{27}Ne, the following assumptions have been made: a $3/2^+$ ground state and a $1/2^+$ excited state at 885 keV, as suggested by the shell model predictions. A 765 keV excited state is sketched as a single particle negative parity state X^-. Two possibilities are computed: a $\Delta l = 3$ state (case a of Table 1) and a $\Delta l = 1$ state (case b) neutron transfer reaction, respectively. The spectroscopic factors concerning the positive parity states are obtained from the USD interaction and the ANTOINE [28,29] shell model code. The experimental reduced transition probability $B(E2; 0^+_{gs} \rightarrow 2^+)(^{26}$Ne) [30] is used for the Coulomb coupling between ^{26}Ne$_{gs}$ and ^{26}Ne(2^+) and for an estimate of the nuclear deformation length, assuming a radius of $1.2 \times 26^{1/3}$ fm. The X^+ states of ^{27}Ne are considered to be pure single particle states with spectroscopic factors fixed to 1. The entrance ^{26}Ne $+ d$ and exit ^{27}Ne $+ p$ channel potentials are obtained from the nucleon-nucleus global potential of [31]. The calculations take into account the variation of cross section due to the target thickness, and the 2.7°_{lab} angular acceptance of VAMOS. The results are compared to experimental values in Table 1 where experimental and USD spectroscopic factors are also gathered. The calculated cross sections are estimated within a 20–30% uncertainty due to the choice of the radius parameter, taken as $1.2 \times 26^{1/3}$ fm, in the ^{26}Ne $+ n$ binding potential and to the unperfect knowledge of the entrance an exit channel potentials. The uncertainties on the experimental spectroscopic factors C^2S essentially come from the uncertainties on experimental cross sections, on the branching ratio τ between the two excited states and on the calculation of cross sections, as previously discussed. The calculated cross sections with the above assumptions reproduce the experimental trend: a poorly populated 885 keV state and a more strongly populated 765 keV state, which is consistent with the selectivity of (d, p) reactions, expected to strongly populate single particle states. The cross section of the first excited state (765 keV) is in agreement with the hypothesis of a negative parity single particle state, either $\Delta l = 1$ or $\Delta l = 3$ with a spectroscopic factor $C^2S = 0.6(2)$. The experimental spectroscopic factor $C^2S = 0.2(2)$ for the ground state of ^{27}Ne is smaller than the USD prediction $C^2S = 0.64$. This difference may come from a contribution of the fp shell in the ^{27}Ne ground state wave function, not taken into account in USD calculations. The spectroscopic factors are obtained from the CDCC formalism in order to reproduce the experimental integrated cross sections. Concerning the 765 keV state, no strong difference for C^2S is observed between $\Delta l = 1$ and $\Delta l = 3$ cases. The low-lying fp shell orbits, suggested for ^{29}Mg [9,10] and observed in this work for ^{27}Ne, can have two origins: a smaller spherical energy gap between the d$_{3/2}$ subshell and the fp shell [4,5,32] and/or deformation [8,33].

In conclusion, we performed the γ spectroscopy of ^{27}Ne using the one-neutron transfer reaction ^{26}Ne$(d, p)^{27}$Ne in inverse kinematics at 9.7 MeV/nucleon. Two bound excited states for

^{27}Ne were observed at 765 keV and 885 keV. Measured with the selective (d, p) reaction, the 765 keV state is consistent with a negative parity state and a spectroscopic factor $C^2 S = 0.6(2)$. These new data confirm a decrease of the negative parity state energies in odd $N = 17$ neutron rich isotones (see Fig. 1), supporting a reduced sd–fp shell gap.

Acknowledgements

The authors would like to thank the SPIRAL beam delivery team, and the EXOGAM, VAMOS and cryogenic technical staffs for their essential and excellent support.

References

[1] C. Détraz, et al., Phys. Rev. C 19 (1979) 164.
[2] T. Motobayashi, et al., Phys. Lett. B 346 (1995) 9.
[3] M. Beiner, R.J. Lombard, D. Mas, Nucl. Phys. A 289 (1975) 1.
[4] T. Otsuka, et al., Phys. Rev. Lett. 87 (2001) 082502.
[5] A. Obertelli, et al., Phys. Rev. C 71 (2005) 024304.
[6] A. Ozawa, et al., Phys. Rev. Lett. 84 (2000) 5493.
[7] M. Stanoiu, et al., Phys. Rev. C 69 (2004) 034312.
[8] A.P. Zuker, Phys. Rev. Lett. 91 (2003) 179201.
[9] L.K. Fifield, et al., Nucl. Phys. A 437 (1985) 141.
[10] P. Baumann, et al., Phys. Rev. C 39 (1989) 626.
[11] V. Tripathi, et al., Phys. Rev. Lett. 94 (2005) 162501.
[12] Y. Utsuno, et al., Phys. Rev. C 70 (2004) 044307.
[13] M. Belleguic-Pigeard de Gurbert, PhD thesis, Université Claude Bernard-Lyon I, IPN Orsay, 2000.
[14] H. Iwasaki, et al., Phys. Lett. B 620 (2005) 118.
[15] P. Dolégiéviez, et al., Report GANIL A 00 01, 2000.
[16] R. Anne, in: E. Penionzhkevich, E.A. Cherepanov (Eds.), Proceedings of EXON 2001, World Scientific, 2001;
H. Savajols, VAMOS Collaboration, Nucl. Phys. A 654 (1999) 1027c.
[17] http://www.ganil.fr/exogam.
[18] GEANT, CERN, Geneva, 1993.
[19] G. Audi, et al., Nucl. Phys. A 729 (2003) 337.
[20] R. Terry, private communication, 2005.
[21] B.A. Brown, B.H. Wildenthal, Annu. Rev. Nucl. Part. Sci. 38 (1988) 29.
[22] L. Weissman, et al., Phys. Rev. C 70 (2004) 057306.
[23] M.W. Cooper, et al., Phys. Rev. C 65 (2002) 051302R.
[24] Y. Utsuno, et al., Phys. Rev. C 60 (1999) 054315.
[25] T. Otsuka, Y. Utsuno, private communication, 2005.
[26] I.J. Thompson, Comput. Phys. Rep. 7 (1988) 167.
[27] N. Keeley, N. Alamanos, V. Lapoux, Phys. Rev. C 69 (2004) 064604.
[28] E. Caurier, Shell model code ANTOINE, IRES, Strasbourg 1984–2004.
[29] E. Caurier, F. Nowacki, Acta Phys. Pol. 30 (1999) 705.
[30] B.V. Pritychenko, et al., Phys. Lett. B 461 (1999) 322.
[31] A.J. Koning, J.P. Delaroche, Nucl. Phys. A 713 (2003) 231.
[32] Y. Utsuno, et al., Phys. Rev. C 64 (2001) 011301(R).
[33] P. Federman, S. Pittel, Phys. Lett. B 69 (1977) 385.